

Supplementary Information

DMSO-modified porous organogel with breathability and degradability for wearable electronics

Zijun Ye,^{‡*a*} Hao Lei,^{‡*a*} Peixuan Zhang,^{‡*a*} Yingying Liu,^{‡*a*}, Yina Liu^{*b*}, Jun Cao^{*c*}, Zhen Wen^{*a*}, Jiwei Jiang,^{**a*} Bin Dong,^{**a*} and Xuhui Sun^{**a*}

^{*a*} Institute of Functional Nano and Soft Materials (FUNSOM), Jiangsu Key Laboratory for Carbon-Based Functional Materials and Devices Soochow University, 199 Ren'ai Road, Suzhou, Jiangsu, 215123, P.R. China.

^{*b*} Department of Applied Mathematics, School of Mathematics and Physics, Xi'an Jiaotong-Liverpool University, Suzhou, 215123, P.R. China

^{*c*} School of Geography, Geomatics and Planning, Jiangsu Normal University, Xuzhou, P.R. China.

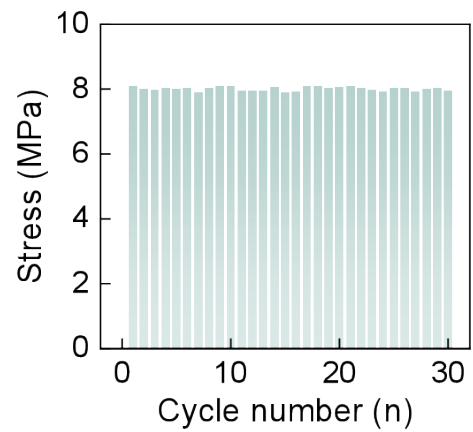


Fig. S1. Strain strength of DSAO under 30 cycles of 1.8% tensile loading

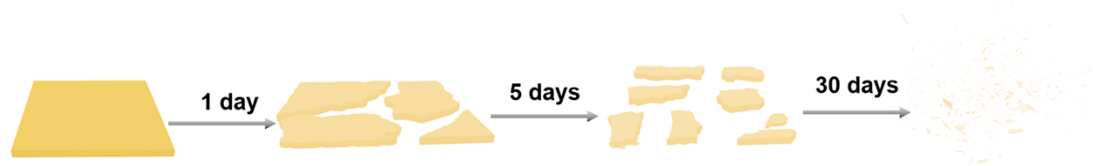


Fig. S2. Schematic diagram of degradation.

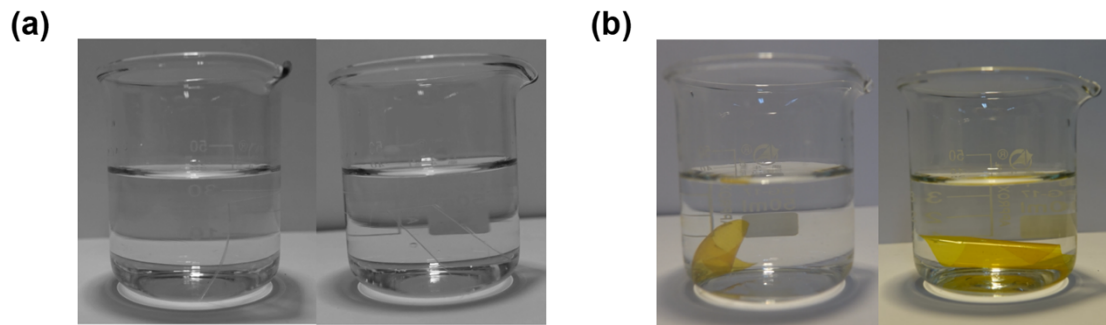


Fig. S3. CCD images of (a)PET, (b)PI after placement in hydrochloric acid solution for 0 and 30 days.

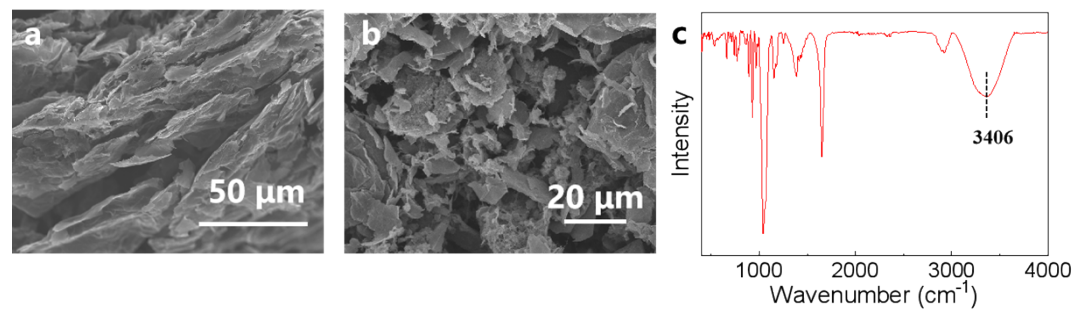


Fig. S4. SEM images of grapheme/DSAO (a) section and (b) surface. (c) The Fourier transform infrared spectroscopy of grapheme/DSAO.

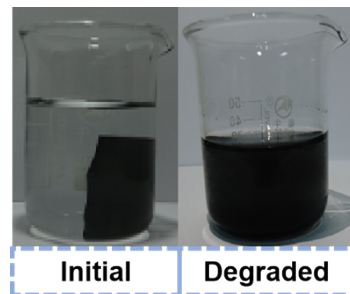


Fig. S5. CCD images of graphene/DSAO after placement in hydrochloric acid solution for 0 and 30 days.

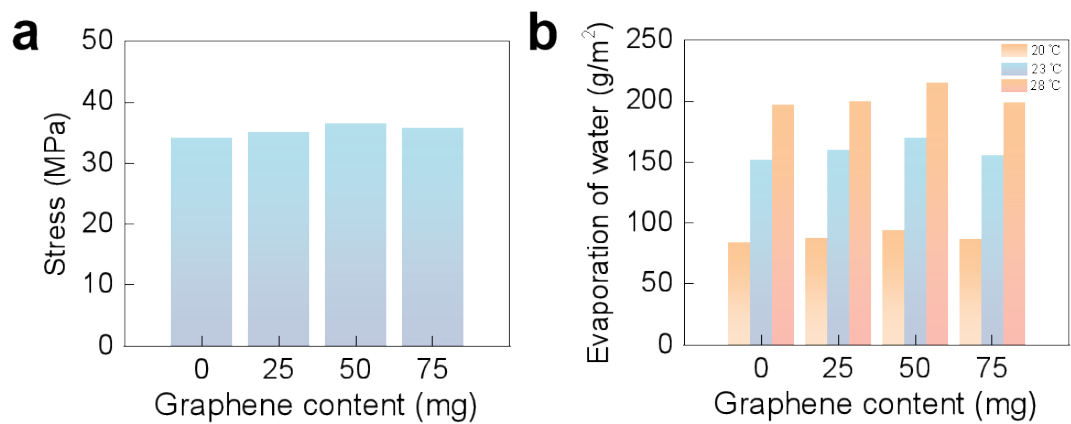


Fig. S6. (a) Breaking strength and (b) air permeability of DSAO with different graphene additions.

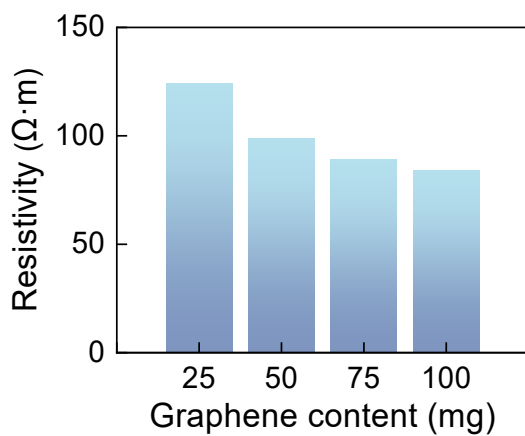


Fig. S7. DSAO resistivity at different graphene content.



Fig. S8. CCD image of active layer of TENG.

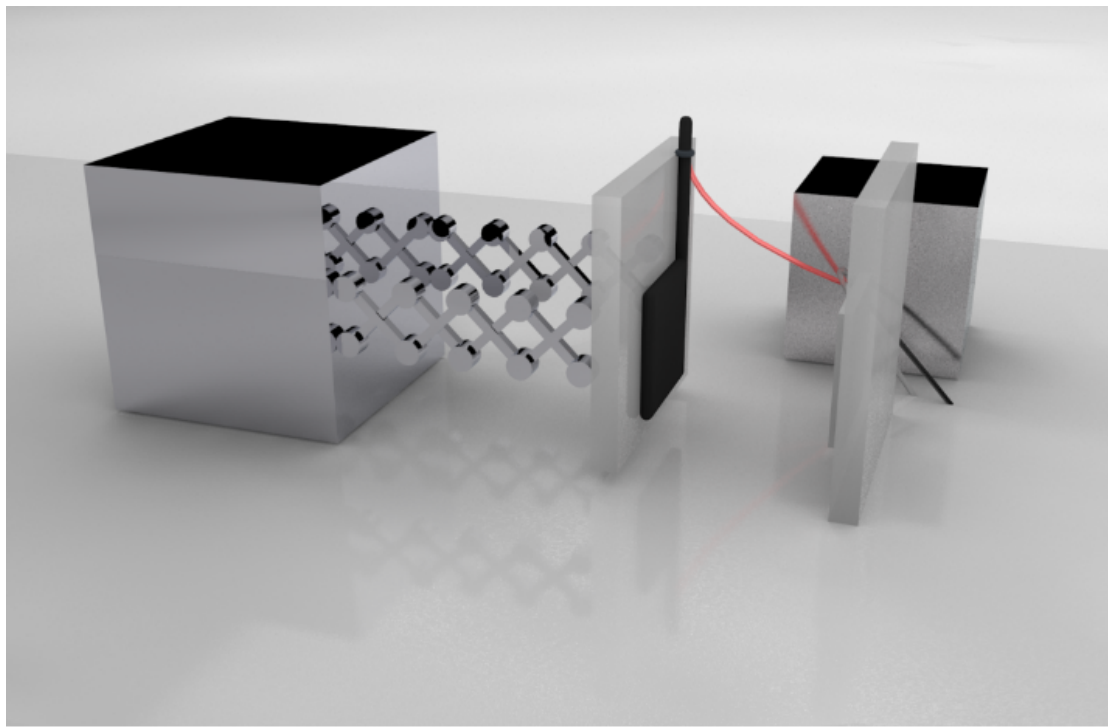


Fig. S9. Schematic diagram of TENG testing platform.

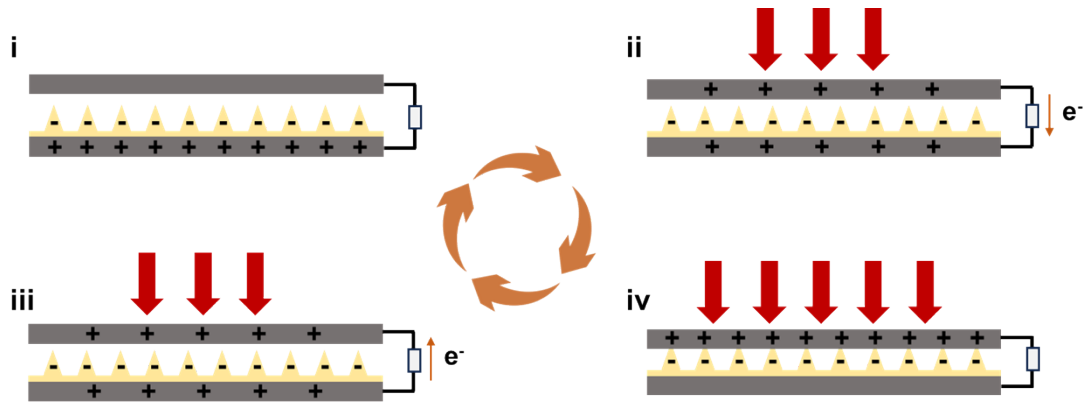


Fig. S10. Working mechanism of the TENG under compressive deformation.

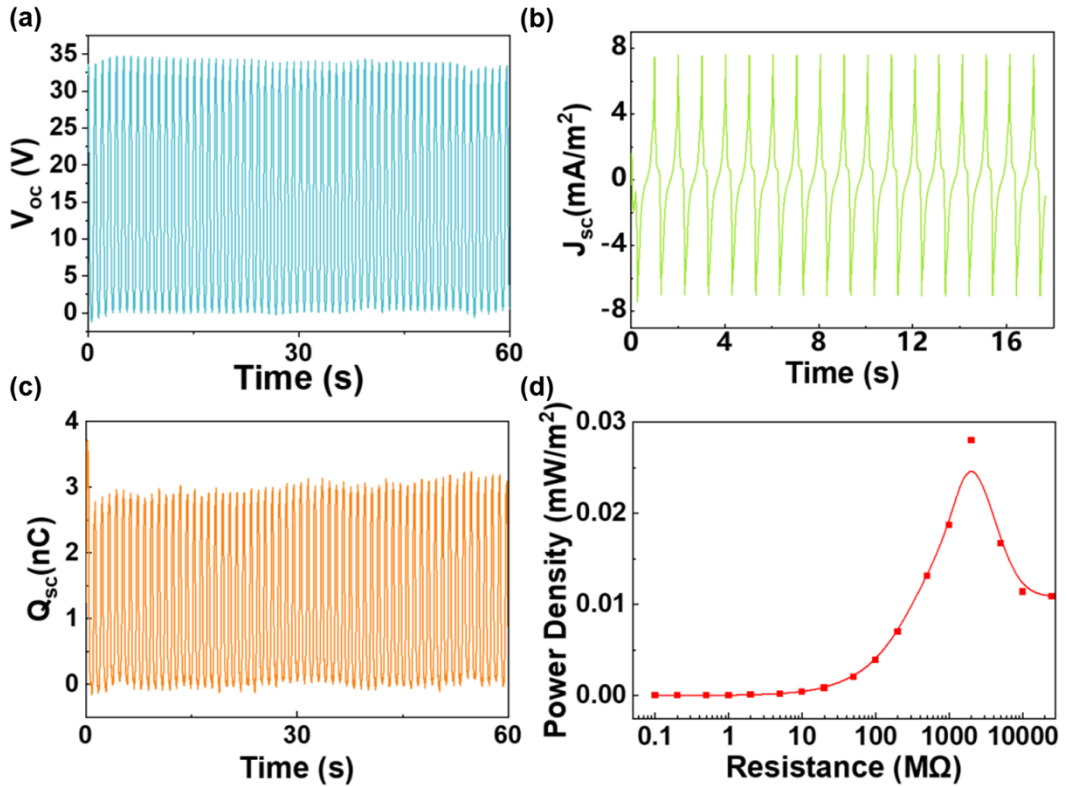


Fig. S11. Output characteristics of the TENG. (a) Voltage cycle under the certain pressure, which indicates the good stability. (b) Current density of the TENG, highlighting the potential in energy harvesting applications. (c) Charge cycle of the TENG. (d) Power density under different load resistances, where the peak value occurs at $1200\text{ M}\Omega$.

Table S1. The mechanical properties in the literatures

	Tensile strength (MPa)	Young's modulus (MPa)	Ref.
Ag-LM-PVA organogel	0.0171	0.02	S1
PVA-LN organogel	1.28	0.52	S2
NVP-HA organogel	0.41	0.8	S3
PAAm organogel	0.025	0.007	S4
(C ₃₈ H ₃₄ P ₂) MnBr ₄ organogel	0.072	0.031	S5

Table S2. The water vapor transmission rate in the literatures

	water vapor transmission rate (g/m ²)	Ref.
illite-PE organogel	13.271	S6
LCNFs organogel	62	S7
PEN organogel	0.58	S8
PTFE organogel	148	S9

Reference

- S1. Y. Zhao, Y. Ohm, J. Liao, Y. Luo, H.-Y. Cheng, P. Won, P. Roberts, M. R. Carneiro, M. F. Islam, J. H. Ahn, L. M. Walker and C. Majidi, *Nat. Electron.*, 2023, **6**, 206-215.
- S2. Y. Feng, J. Yu, D. Sun, W. Ren, C. Shao and R. Sun, *Chem. Eng. J.*, 2022, **433**, 133202.
- S3. J. Ma and S. Wen, *Chem. Eng. J.*, 2023, **470**, 144264.
- S4. Y.-F. Liu, Q. Liu, J.-F. Long, F.-L. Yi, Y.-Q. Li, X.-H. Lei, P. Huang, B. Du, N. Hu and S.-Y. Fu, *ACS Appl. Mater. Interfaces*, 2020, **12**, 49866-49875.
- S5. L. Liu, H. Hu, W. Pan, H. Gao, J. Song, X. Feng, W. Qu, W. Wei, B. Yang and H. Wei, *Adv. Mater.*, 2024, **36**, 2311206.
- S6. D. M. Seong, H. Lee, J. Kim and J. H. Chang, *Materials*, 2020, **13**, 2382.
- S7. X. Gu, W. Wang, J. Kang, X. Dong, P. Guan and B. Li, *Small*, 2025, 2407438.
- S8. J. C. Bi, J.-Y. Park, S. Lee, S. Park, J. Song, J.-S. Lee, K.-C. Kang, K. Kim, D. Lim, Y. W. Park and B.-K. Ju, *ACS Appl. Mater. Interfaces*, 2025.
- S9. T. Li, Y. Ding, C. Teng, Y. Zheng, X. Wang and D. Zhou, *ACS Appl. Mater.*

Interfaces, 2024, **16**, 60625-60632.